Journal of Biomedical Optics

BiomedicalOptics.SPIEDigitalLibrary.org

In vivo characterization of colorectal metastases in human liver using diffuse reflectance spectroscopy: toward guidance in oncological procedures

Jarich W. Spliethoff
Lisanne L. de Boer
Mark A. J. Meier
Warner Prevoo
Jeroen de Jong
Koert Kuhlmann
Torre M. Bydlon
Henricus J. C. M. Sterenborg
Benno H. W. Hendriks
Theo J. M. Ruers

Jarich W. Spliethoff, Lisanne L. de Boer, Mark A. J. Meier, Warner Prevoo, Jeroen de Jong, Koert Kuhlmann, Torre M. Bydlon, Henricus J. C. M. Sterenborg, Benno H. W. Hendriks, Theo J. M. Ruers, "*In vivo* characterization of colorectal metastases in human liver using diffuse reflectance spectroscopy: toward guidance in oncological procedures," *J. Biomed. Opt.* **21**(9), 097004 (2016), doi: 10.1117/1.JBO.21.9.097004.

SPIE.

In vivo characterization of colorectal metastases in human liver using diffuse reflectance spectroscopy: toward guidance in oncological procedures

Jarich W. Spliethoff,[a,*] Lisanne L. de Boer,[a] Mark A. J. Meier,[b] Warner Prevoo,[b] Jeroen de Jong,[c] Koert Kuhlmann,[a] Torre M. Bydlon,[d] Henricus J. C. M. Sterenborg,[e] Benno H. W. Hendriks,[d] and Theo J. M. Ruers[a,f]
[a]Netherlands Cancer Institute, Department of Surgery, Plesmanlaan 121, 1066CX Amsterdam, The Netherlands
[b]Netherlands Cancer Institute, Department of Radiology, Plesmanlaan 121, 1066CX Amsterdam, The Netherlands
[c]Netherlands Cancer Institute, Department of Pathology, Plesmanlaan 121, 1066CX Amsterdam, The Netherlands
[d]Philips Research, Department In-body Systems, High Tech Campus 34, 5656AE Eindhoven, The Netherlands
[e]Academic Medical Center, Department of Biomedical Engineering and Physics, Meibergdreef 9, 1105AZ Amsterdam, The Netherlands
[f]University of Twente, MIRA Institute, Drienerlolaan 5, Zuidhorst ZH116, 7522 NB Enschede, The Netherlands

Abstract. There is a strong need to develop clinical instruments that can perform rapid tissue assessment at the tip of smart clinical instruments for a variety of oncological applications. This study presents the first *in vivo* real-time tissue characterization during 24 liver biopsy procedures using diffuse reflectance (DR) spectroscopy at the tip of a core biopsy needle with integrated optical fibers. DR measurements were performed along each needle path, followed by biopsy of the target lesion using the same needle. Interventional imaging was coregistered with the DR spectra. Pathology results were compared with the DR spectroscopy data at the final measurement position. Bile was the primary discriminator between normal liver tissue and tumor tissue. Relative differences in bile content matched with the tissue diagnosis based on histopathological analysis in all 24 clinical cases. Continuous DR measurements during needle insertion in three patients showed that the method can also be applied for biopsy guidance or tumor recognition during surgery. This study provides an important validation step for DR spectroscopy-based tissue characterization in the liver. Given the feasibility of the outlined approach, it is also conceivable to make integrated fiber-optic tools for other clinical procedures that rely on accurate instrument positioning. [DOI: 10.1117/1.JBO.21.9.097004]

Keywords: diffuse reflectance spectroscopy; fiber-optic; tissue diagnosis; liver; tumor.

Paper 160478R received Jul. 8, 2016; accepted for publication Aug. 30, 2016; published online Sep. 16, 2016.

1 Introduction

The emergence of minimally invasive diagnostic and interventional procedures has increased the demand for real-time guidance for a variety of oncology applications that rely on accurate instrument positioning and procedural feedback. To this aim, optical spectroscopy has been investigated as a tool to increase the accuracy and efficacy of clinical procedures.

As spectroscopy measurements can be conducted through thin needles (28 G; 0.36 mm),[1] there is a strong rationale to perform optical spectroscopy measurements at the tip of a needle for rapid tissue characterization. This can be used for biopsy guidance by providing more selective tissue acquisition[2] and increasing the diagnostic yield and biopsy quality.[3] The development of advanced needles for needle-based thermal therapies, such as radiofrequency ablation, microwave ablation, and cryoablation in the liver, has offered minimally invasive therapies to patients that were previously untreatable. The success of these treatments is highly dependent on the accurate placement of the ablation needles, therefore, tissue characterization at the tip of the device would be of significant value.[4–6] The functionality of optical spectroscopy added to a surgical instrument could help surgeons to find the optimal resection plane and ensure completeness of tumor removal, as the recognition of the tumor tissue during surgery is often challenging,[7] especially in minimally invasive procedures.

Diffuse reflectance (DR) spectroscopy is a widely used technique to estimate the optical properties of tissue where tissue is illuminated with a selected spectral band of light. The light is either scattered or absorbed by the tissue, depending on the specific composition of the tissue. Subsequent analysis of the tissue's spectral response provides specific quantitative morphologic, biochemical, and functional information, thereby enabling tissue discrimination and potentially improving diagnostic capability.

Several preclinical studies were performed in the last decade showing the potential of DR spectroscopy to discriminate liver tumors and surrounding liver tissue.[1,8–10] Nachabé et al.[8,9] investigated differences between healthy tissue and metastatic tumor from *ex vivo* human liver specimens using diffuse optical spectroscopy with a fiber optic probe. It was shown that bile should be included when analyzing DR liver data because of its presence in the liver bile ducts and its strong optical signature.[8] In a preclinical (*ex vivo*) study by Evers et al.,[9] bile content was found to be significantly higher in normal liver tissue compared to colorectal liver metastases. In addition to bile, the main chromophore in liver tissue dominating the absorption in the visible spectrum (400 to 750 nm) is hemoglobin (oxygenated and deoxygenated).[8,11] Water and fat dominate in the near-infrared range (>800 nm).[8,12,13] The main scattering parameters in liver tissue are the reduced scattering at 800 nm and the Mie-to-total

*Address all correspondence to: Jarich W. Spliethoff, E-mail: j.spliethoff@nki.nl

1083-3668/2016/$25.00 © 2016 SPIE

scattering fraction, in which the total scattering of tissue is assumed to be defined by Mie and Rayleigh scattering.[8,9] In previous *ex vivo* studies on 14 and 24 resection specimen on average, a lower reduced scattering (at 800 nm) was found in colorectal liver metastases in comparison with healthy liver tissue.[8,9]

A considerable challenge in DR spectroscopy-based tissue characterization during clinical procedures (e.g., needle guidance and surgical guidance) is the inevitable presence of blood. Earlier it was shown that extending the measurement into the near-infrared region up to 1600 nm, where blood has no significant absorption features, helps to overcome the effect of dominant absorption by excessive amounts of hemoglobin in the visible wavelength region (400 to 700 nm) that can occur due to bleeding. Whether bile, which is strong absorber in the visible wavelength range, can still be measured accurately under specific operating constraints in the clinic (e.g., when considerable amounts of blood are encountered) has not been elucidated.

Histology remains the gold-standard for diagnosis and staging in oncology, making it in essence a ground truth for new technologies attempting to measure and quantify these pathologies. However, clinical validation studies are often confounded by imperfect spatial correlation of the optical reading and the tissue sample removed for histopathological analysis.[14,15] An approach to address discrepancies between spectral data and histology is to integrate fiber-optics into standard tissue-sampling tools such as a core biopsy needle, thereby linking spectroscopy and biopsy functionality in a single instrument.[2] This feature guarantees a near-perfect match between optically sampled and histologically analyzed tissue.

The objective of the present study is to assess the *in vivo* tissue discriminating abilities of DR spectroscopy in a series of image-guided liver biopsy procedures using a core biopsy needle with integrated optical fibers.

2 Materials and Methods

2.1 *Study Setup*

The protocols for the clinical study were reviewed and approved by the institutional review board of The Netherlands Cancer Institute—Antoni van Leeuwenhoek Hospital. The study was registered at the Netherlands Trial Register (NTR3651) and the U.S. National Institutes of Health Clinical Trial Database (NCT01730365). Patients scheduled for a regular core needle biopsy for a suspected liver malignancy and patients undergoing a percutaneous liver radiofrequency ablation were recruited for study participation. The lesions were required to be greater than 1 cm, located in the liver tissue at least 1 cm from the liver surface, and had to be safely accessible. Patients at increased risk of bleeding were excluded. All patients gave written informed consent prior to the experimental procedures.

2.2 *Image Guidance and Data Acquisition*

The radiologist identified the liver lesion of interest by either computed tomography (CT)-fluoroscopy or ultrasound imaging according to standard protocol. The fiber-optic biopsy needle (FOBN) was inserted at the planned entry point and DR measurements were performed along the needle tract, followed by DR measurements and biopsy of the target lesion using the same needle. A total of 24 lesions in 21 patients were analyzed. In the first 18 patients, sets of 3 to 5 DR spectra were acquired at discrete locations in (1) normal liver tissue, (2) tissue at the tumor border, and (3) tumor tissue. For each patient, the FOBN was fired immediately after final DR measurements to obtain a physical tissue sample from the target lesion. In three patients, near-real-time DR measurements were taken in rapid succession (interval ~1 s) along the needle tract. Imaging was performed simultaneously with DR spectroscopic acquisition to allow registration of the DR measurements with the location of the needle tip.

2.3 *Tissue Processing*

The distal end of the tissue samples was marked with yellow tissue marking dye (Polysciences Inc., Warrington, United Kingdom) for orientation purposes. The samples were formalin-fixed and processed according to routine histopathology. After paraffin embedding, the samples were sectioned and stained with standard hematoxylin and eosin (Merck, Darmstadt, Germany). The resulting tissue slices were examined by light microscopy by an experienced pathologist, who was blinded to the spectroscopic findings. The glass slides were digitized by a histologic slide scanner (ScanScope—Aperio Technologies Inc., Vista, California). Pathology results were compared with the DR spectroscopy data at the final measurement position. Normal positions were assumed to be histologically normal liver tissue and border locations a mixture of normal liver tissue and tumor.

2.4 *Portable Spectroscopy System and Fiber-Optic Biopsy Needle*

The general principles of DR spectroscopy, the operating features of the spectroscopy system, and the calibration procedure have been described elaborately by Nachabé et al.[12,13] The system consists of a tungsten halogen broadband light source (360 to 2500 nm) with an embedded shutter, two spectrometers: one which resolves the light in the visible wavelength range, i.e., 400 up to 1100 nm (Andor Technology, DU420ABRDD) and another one which resolves near-infrared light from 900 up to 1700 nm (Andor Technology, DU492A-1.7). The 16-G FOBN (Invivo Germany, Schwerin, Germany) consists of one 100-μm diameter fiber for light delivery and two identical adjacent fibers with a diameter of 200 μm for the collection of the reflected light (one fiber for each spectrometer). The distance between the emitting and collecting fibers at the needle tip was 1.36 mm, resulting in a tissue probing depth of ~1 to 2 mm.

In the FOBN, DR spectroscopy and biopsy functionality are linked in a single instrument, which allows registration of optical measurements with histology.[2] The calibration of the spectroscopy system prior to tissue measurements consisted of several steps, including calibrating the system with a white reflectance standard measurement to correct for system response (spectral variations of the light source, spectrometer, fiber transmission, and so on).[12,13] For the *in vivo* studies, the spectroscopy system was calibrated for system response by measuring reflectance from a spectrally flat barium sulfate casing around a non-sterile calibration needle. After the calibration, the calibration needle was disconnected and the sterile-packaged fiber-optic needle was connected for the tissue measurements.

2.5 *Spectral Data Analysis*

DR measurements were spectrally fit with an analytical model by Farrell et al.[16] that was derived from diffusion theory using a trust region nonlinear inversion algorithm to determine the

Table 1 Demographics and individual data for patients ($n = 21$).

Patient number	Gender	Age (yr)	Lesion number.	Tumor diameter (mm)	Relative tumor bile content	Histopathology
1	Female	83.7	1	21	↓ (0.51)	Metastasis colon carcinoma (partly necrotic)
2	Female	65.9	1	31	↓ (0.27)	Metastasis colon carcinoma
3	Male	64.8	1	22	↓ (0.56)	Metastasis neuroendocrine tumor
			2	25	↓ (0.68)	Metastasis neuroendocrine tumor
4	Male	55.3	1	19	↓ (0.00)	Metastasis colon carcinoma (partly necrotic)
5	Male	65.8	1	15	↓ (0.54)	—
6	Female	66.9	1	20	↓ (0.72)	Metastasis rectum carcinoma
7	Female	80.5	1	26	↓ (0.38)	Metastasis breast carcinoma
8	Male	56.6	1	55	↓ (0.04)	Metastasis colon carcinoma (partly necrotic)
9	Female	67.0	1	13	↑ (1.30)	Nondiagnostic; only liver tissue
10	Female	55.7	1	11	↑(1.11)	Nondiagnostic; only liver tissue
11	Male	65.4	1	13	↓ (0.45)	Metastasis colon carcinoma
12	Male	57.9	1	35	↓ (0.16)	Metastasis colon carcinoma (partly necrotic)
			2	40	↓ (0.01)	Metastasis colon carcinoma (partly necrotic)
13	Male	75.5	1	52	↓ (0.23)	Metastasis colon carcinoma (partly necrotic)
14	Female	65.4	1	28	↓ (0.37)	—
15	Female	69.9	1	25	↓ (0.12)	Metastasis colon carcinoma (partly necrotic)
16	Male	71.4	1	24	↓ (0.17)	Metastasis colon carcinoma
17	Female	64.7	1	42	↓ (0.17)	Metastasis rectum carcinoma (partly necrotic)
18	Male	80.2	1	45	↓ (0.52)	Metastasis colon carcinoma
			2	71	↓ (0.14)	Metastasis colon carcinoma (partly necrotic)
19	Male	69.5	1	42	↓ (0.25)	Metastasis colon carcinoma (partly necrotic)
20	Female	48.1	1	47	↓ (0.01)	Metastasis rectum carcinoma (partly necrotic)
21	Female	68.3	1	34	↓ (0.04)	Metastasis colon carcinoma (mainly fibrotic)
Median (range)		65.9 (48.1 to 83.7)		27 (11 to 71)		

absorption coefficient $\mu_a(\lambda)$ and the reduced scattering coefficient $\mu_s(\lambda)$ expressed in cm^{-1}. The validation of the model, including spectral calibration procedures, and its application in various preclinical studies were described in detail elsewhere.[9,17–19] The model uses prior knowledge of light–tissue interaction to translate the acquired spectra into estimates of various absorption and scattering parameters, such as biological volume fractions (e.g., blood, bile, water, and fat), oxygenation level of blood [stO_2], and the reduced scattering coefficient at 800 nm [$\mu_s'(800)$].

2.6 *Statistics*

Based on histopathological analysis and procedural imaging, the DR measurements were classified as normal liver tissue, tumor border, or tumor. Tissue parameters determined from DR measurements [e.g., blood, stO_2, bile, $\mu_s'(800)$, water, and fat] were compared between these tissue categories using a generalized estimating equation (GEE) approach thereby taking into account repeated measurements within the same subject. The DR spectroscopy parameters were assumed to be normally distributed. Within-patient dependencies were represented by the correlation matrix where all pairwise correlations were assumed to be equal (equicorrelated). The analyses were performed using the GEEQBOX toolbox in MATLAB® 8.4 (MathWorks Inc., Natick, Massachusetts) and $p < 0.01$ was considered statistically significant. Receiver operating characteristics (ROC) curves and corresponding area-under-the-curve (AUC) values were calculated to evaluate the diagnostic value of individual DR spectroscopy parameters. To verify the

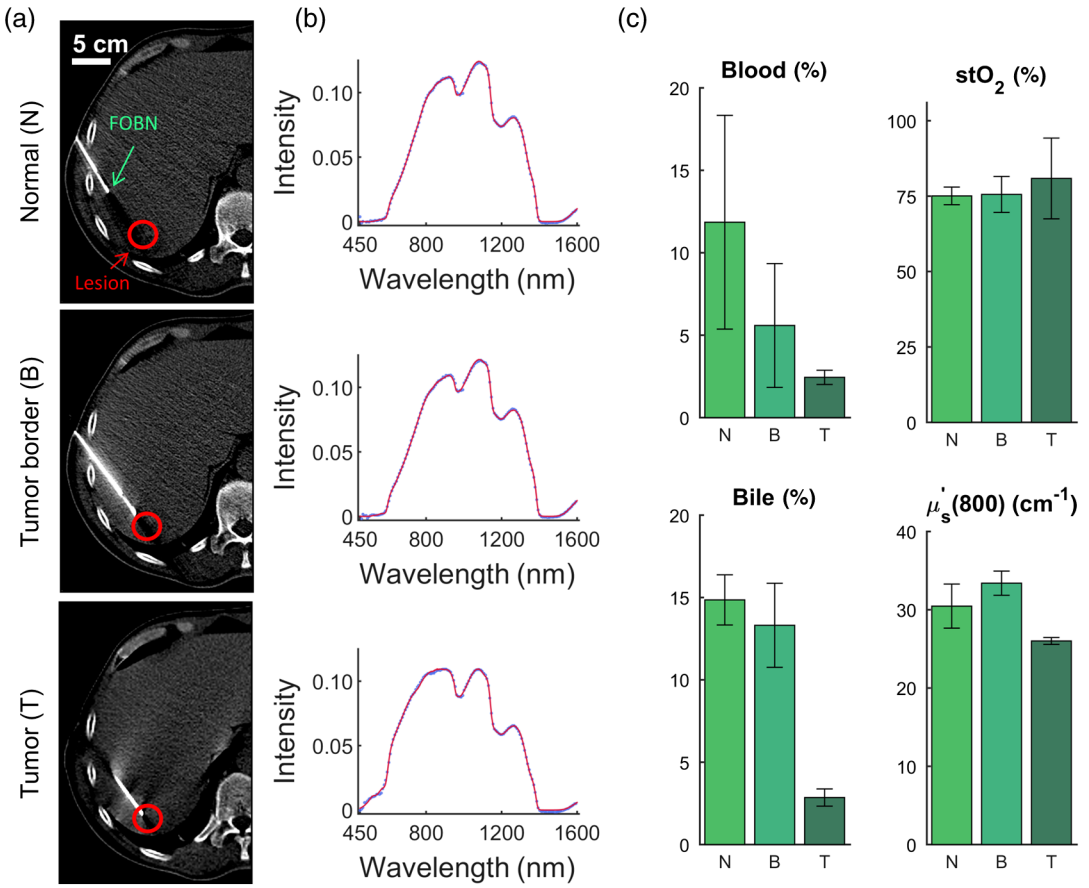

Fig. 1 Example of added quantitative spectral functionality during routine liver biopsy (first patient 12 in Table 1). (a) Positioning of the FOBN based on CT-fluoroscopic imaging in liver tissue, at the border of the target lesion and in the target lesion prior to biopsy. (b) Coregistered DR measurements (blue dotted line) and corresponding fit curves (red lines). (c) Data for blood, stO_2, bile, and $\mu_s'(800)$ represent mean values ± standard deviations. N, normal liver tissue; B, tumor border; T, tumor; and FOBN, fiber-optic biopsy needle.

performance of the FOBN per individual, parameter values for blood content, stO_2, bile content, and μ_s' (800) were scaled to the average values measured within normal liver tissue of each patient, thereby using each patient's normal liver tissue as an internal reference.

3 Results

Of the 21 patients, the median age was 65.9 yr (range 48.1 to 83.7 yr). Eleven participants (52%) were women. The median tumor size was 27 mm (range 11 to 71 mm). Histopathological examination of the targeted tissue revealed 20 malignancies, of which 17 were classified as metastasis from colorectal adenocarcinomas (Table 1). One tumor was identified as a metastasis from a breast tumor and two lesions were metastases of a neuroendocrine tumor. Two biopsies yielded only nondiagnostic material (subjects 9 and 10). In two patients (subjects 5 and 14), there was a mismatch between final DR measurement position and biopsy location due to needle movement after the final DR measurements. For these patients, DR recordings were only linked to the imaging and not with tissue classification based on histology.

3.1 *Cohort Analysis*

Figure 1 illustrates how DR tissue characterization was performed using the FOBN. Added real-time spectral measurements did not interfere with the standard biopsy procedure. When the collective data ($n = 333$ DR spectra) were compared (Fig. 2), significant compositional differences ($p < 0.01$) between tumor tissue and liver tissue were noted for blood, stO_2, bile, and $\mu_s'(800)$. Area under the corresponding ROC curves was used to measure the ability of various DR spectroscopy parameters to discriminate tumor tissue from normal liver tissue (Fig. 2). Blood content, stO_2, and $\mu_s'(800)$ demonstrated an AUC of 0.659 to 0.708, indicative of poor to moderate discrimination. Classification based on bile content allowed more accurate identification of tumor tissue (ROC–AUC value: 0.924). The optimum cutoff value of the ROC curve corresponded with a sensitivity of 0.91% and a specificity of 0.88%.

3.2 *Individual Patient Analysis*

Discrimination between various tissues relies on measurement of the absolute or relative differences in intensity or optical contrasts between the tissue types of interest. Sources of variation, such as interpatient variability, may outweigh the difference between the tissue types of interest and lead to hampered diagnostic performance.[9,17,18] Relative changes in DR parameters that occur in a particular insertion may help to define more effective detection criteria that are less sensitive to interpatient variation. Therefore, we determined the relative contrast between

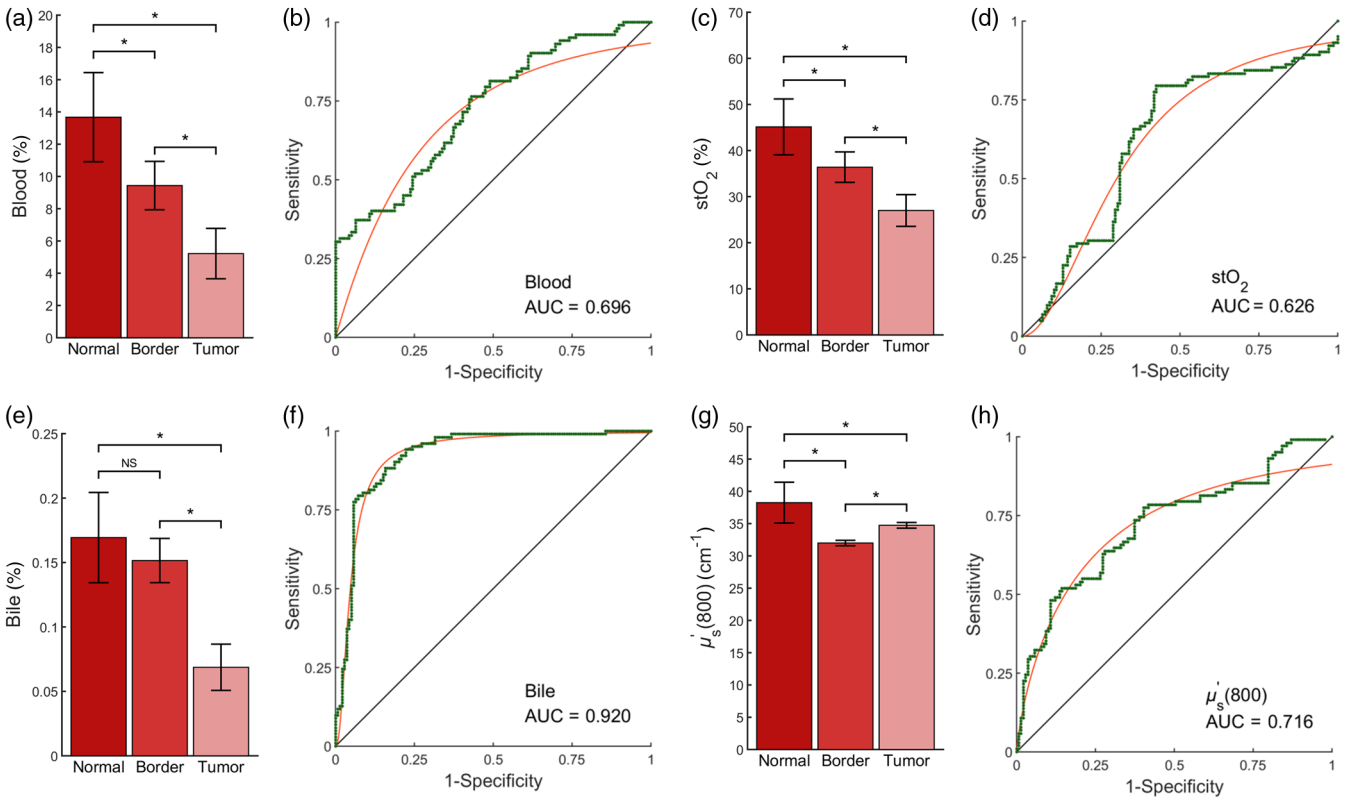

Fig. 2 DR spectroscopy parameter quantification. Bar graphs show the values for (a) blood, (c) stO_2, (e) bile, and (g) $\mu_s'(800)$ as measured in liver tissue (normal), at the tumor border (border) and in the target lesion (tumor). Values are given as mean values ± standard errors, adjusted for repeated measurements. *$p < 0.01$. NS: not significant. Corresponding receiver operating characteristics (ROC) curves (b, d, f, h) indicate the ability to distinguish tumor tissue from liver tissue. AUC: area under ROC curve.

tumor and normal liver tissue based on the spectroscopically derived values for bile content using each patient's normal liver tissue as an internal reference (Fig. 3; Table 1). In 22 out of the 24 biopsy procedures, tumor tissue could be correctly identified based on a decrease in bile content. In the two remaining cases (subject 9 and subject 10), the bile content measured just before biopsy indicated that FOBN was not in contact with the tumor tissue (Fig. 4). In both cases, the histopathological analysis of the biopsy samples confirmed that the targeted lesion was missed. If this feedback had been used, a corrective manipulation of the needle could have increased the chance of an adequate biopsy.

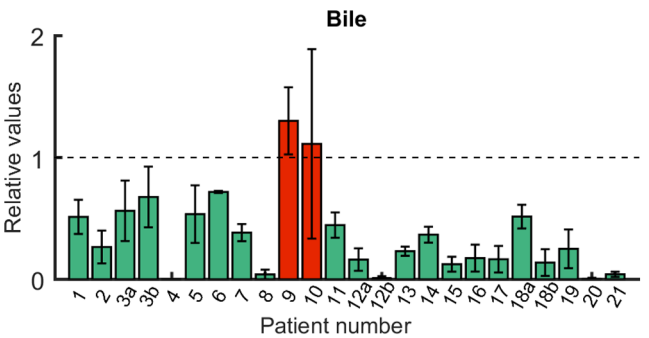

Fig. 3 Relative changes in bile content determined for $n = 24$ insertions. The relative bile content was defined as the bile content in tumor relative to the average value measured in normal liver tissue. Values are given as the mean ± standard deviations. Dotted line: relative bile content = 1.

3.3 *Real-Time Tissue Characterization*

In three patients (subjects 19 to 21), spectral measurements were acquired continuously during needle insertion, as exemplified in Fig. 5. While the needle tip was progressed toward the tumor, CT-fluoroscopic imaging provided the actual location of the needle tip. A decrease in fat content was observed when the tip of the needle was inserted from subcutaneous fat/muscle into the liver. The stO_2 level strongly decreased near the tumor border and in the tumor. Moreover, a clear decrease in bile content was observed once the needle reached the tumor.

4 Discussion

The development of advanced fiber-optic clinical tools could make a significant contribution to diagnosis and treatment monitoring in cancer patients.

The goal of this study was to evaluate the diagnostic potential of DR spectroscopy during image-guided liver biopsy procedures. For this, a core biopsy needle with integrated optical fibers was used to link spectral measurements and biopsy functionality in a single instrument. The use of such an instrument represents a major step forward for clinical evaluation of spectral tissue sensing techniques by greatly increasing the spatial correlation of physical biopsies with spectral measurement spots and simplifying study procedures

Diagnostic performance of our system was tested during 24 image-guided percutaneous liver biopsy procedures. Tissue blood content, bile content, stO_2, and $\mu_s'(800)$ showed statistically significant differences between tumor tissue and surrounding

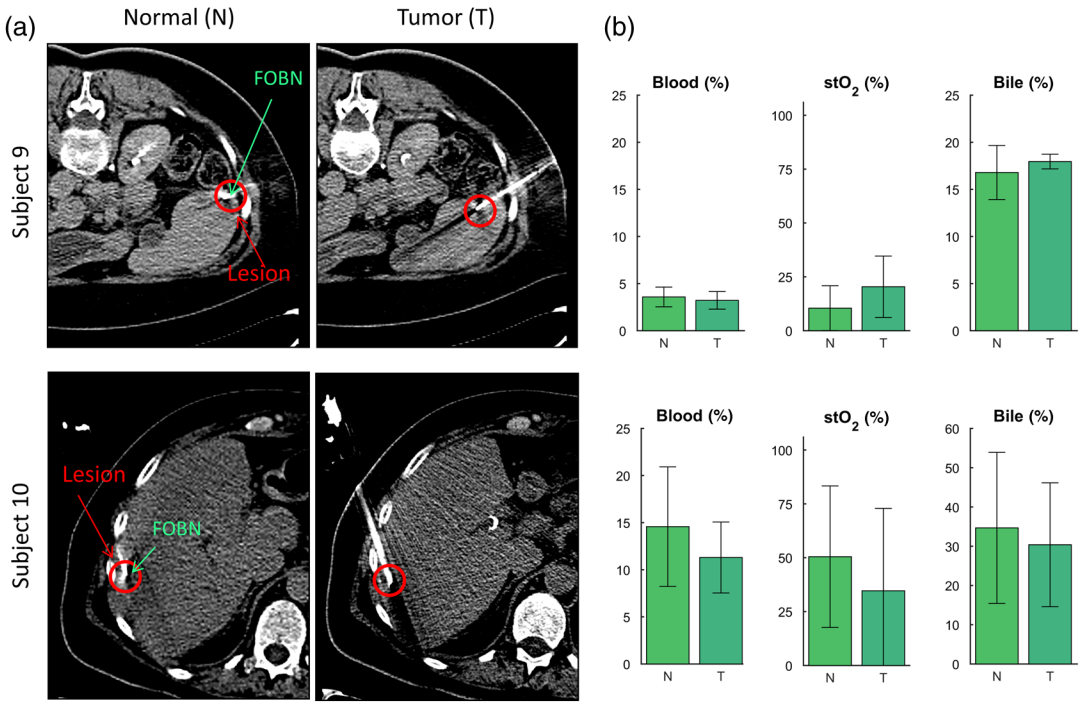

Fig. 4 (a) Although CT-fluoroscopic imaging in subject 9 and subject 10 suggests that the tissue biopsy was taken from the target lesions, the tissue samples proved to be nondiagnostic. The samples contained only normal liver tissue, indicating that the targeted tissue was missed. No substantial change in bile content and other DR spectroscopy parameters was seen. These examples underline the importance of real-time measurements and data analysis in order to identify the transition of needle placement in a tumor based on the changes in the derived parameters. (b) Data for blood, stO_2, and bile represent mean values $\pm$ standard deviations. N, normal lung tissue; T, tumor; and FOBN, fiber-optic biopsy needle.

liver tissue. These findings are consistent with previous preclinical studies.[8–10]

We found that bile content allows accurate discrimination between normal liver tissue and tumor tissue (ROC AUC: 0.924). Relative increases in bile content enabled identification of tumor tissue in all 22 of 24 the clinical cases. In the remaining two cases, DR spectroscopy correctly predicted that the biopsy specimen did not contain tumor tissue. In this series, this corresponds with an overall diagnostic performance of 100%

Normal liver tissue mainly consists of hepatocytes, which are cells that are arranged as very thin plates separated by fine vascular sinusoids where blood flows. Bile produced by liver cells drains into microscopic canals known as bile canaliculi. The lower bile content in secondary liver cancers can be attributed to the loss of the native tissue structure and associated bile perfusion. Whereas bile content is directly linked to tissue structure, the measured blood content is strongly susceptible to bleeding at the tip of the fiber-optic needle.[2] Consequently, estimates for blood content and associated oxygenation levels do not necessarily reflect the true physiologic state of the measured tissue, thus rendering them less suitable for *in vivo* tissue discrimination.

Regarding $\mu_s'(800)$, our results agree with the general reported findings from other (*ex vivo*) human DR spectroscopy studies.[8,9] Liver parenchyma was found to have higher $\mu_s'(800)$ as compared to tumor. This suggests that liver tissue has a larger density of small particles than tumors. This observation collaborates with the fact that healthy liver tissue is rich in densely packed small hepatocytes compared to colorectal liver metastases in the liver. The tissue that is present at the interface between tumor and nontumor tissue strongly depends on the histological growth pattern of such a metastasis.[20] For example, metastases that develop according to a "desmoplastic" or "pushing" growth pattern are separated from surrounding liver parenchyma by a rim of desmoplastic stroma or inflammatory infiltrate, whereas in a "replacement" growth pattern, there is generally no rim or capsule around the metastasis. It is unclear whether the lower values for $\mu_s'(800)$ that were measured with DR spectroscopy at the tumor borders (Fig. 2) are caused either by specific histological characteristics of the tumor or by limitations of the analytical model, which does not take into account multiple layers of tissue.

The information provided by DR spectroscopy, such as mapping of bile levels along the needle path, can be of great relevance in the case of biopsy procedures or other procedures that rely on accurate needle placement. Continuous DR measurements, as performed during this study, may therefore provide additional information with respect to the variation in tissue composition across the tumor as well as identifying the boundaries between normal liver tissue and tumor tissue.

The current experimental system was designed for clinical studies and has proven to be compatible with the existing clinical workflow of percutaneous liver biopsy procedures. Further clinical validation of the outlined approach in a prospective setting or (subsequent) clinical implementation would require that the spectral information is translated into comprehensible and reliable real-time diagnostic information. The optical fiber geometry will be an important consideration for the design of a future fiber-optic tool. For example, probing volume and depth

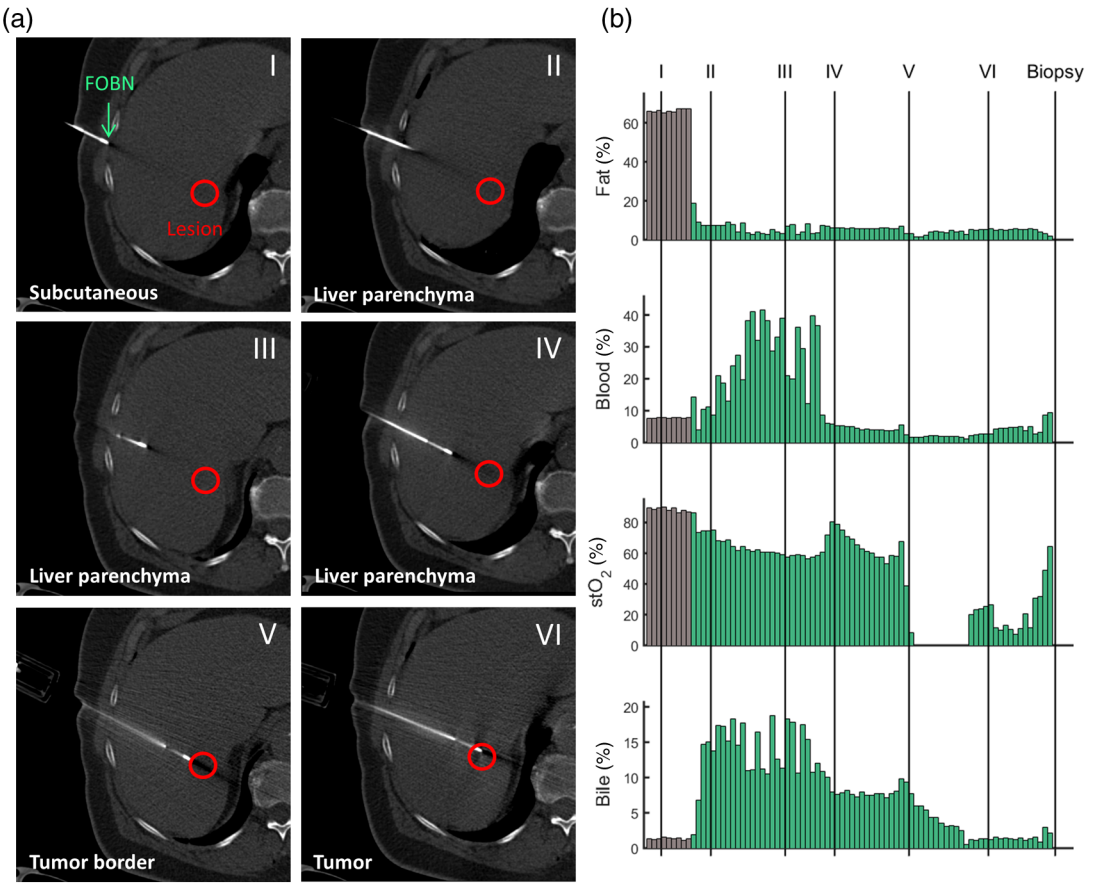

Fig. 5 Real-time tissue characterization and biopsy with the FOBN in an individual. (a) CT-fluoroscopy images during insertion of the FOBN (images I through VI). (b) DR spectroscopy parameters were extracted from the optical data along the needle path. Note that the spectral measurements were started while the FOBN was positioned in subcutaneous fat or muscle. FOBN, fiber-optic biopsy needle.

strongly depend on the tissue's optical properties and the source–detector fiber separation. As the source–detector separation increases, the probing depth and volume increases, which increases the sensitivity of the probe to deeper tissues. However, the ability to detect small amounts of abnormal tissue decreases with a larger probed volume (partial volume effect). The challenge will be to develop a system with a sufficient probing depth and sufficient sensitivity to detect tumor margins or progressive infiltration of tumor into liver parenchyma. Thus, decisions about technical details and the algorithms used for extracting tissue optical properties will be dictated largely by the application needs. This will require further data collection and validation studies.

During biopsy procedures, physicians try to avoid multiple passages to prevent tumor seeding, pain, bleeding, and so on. Continuous real-time DRS measurements, as performed during this study (Fig. 5), can be used to record a profile along the needle path and yield valuable data with respect to the variation in tissue composition across the tumor as well as identifying the boundaries between tissues. Because DR spectroscopy is performed from tissues that are close to the fiber-optic probe tip (1 to 2 mm), we expect that spectral information will ultimately be used complementary to image guidance (e.g., fluoroscopy or ultrasound imaging). By providing crucial information during biopsy needle insertion and just before the tissue sample is taken, the outlined approach may help to reduce the number of false-negative biopsies with minimal impact on routine clinical workflow.

Earlier, we found that the reliability (i.e., confidence intervals) of various DR spectroscopy parameters is not affected by the amount of blood at the fiber-optic probe tip.[2] However, absolute parameter values will depend to some extent on the amount of blood encountered, as blood close to the tip is part of the probed "tissue" volume. The measured blood content at the needle tip—which is accurately quantified—could be provided as feedback to the physician, thereby allowing necessary adjustments of the fiber-optic probe to reduce the effect of blood. Moreover, in the case of surgical guidance, DR spectroscopy is likely to be used in combination with a cauterization instrument. For such an application, an instrument has to be developed that functions reliably in the complex surgical setting. If the instrument is expected to alert the surgeon that tumor tissue is detected, the system must be able to identify any normal or tumor tissue type that could potentially be encountered by the operator during an intervention under all foreseeable operating conditions. Furthermore, surgeons often use electrocauterization to cut through soft tissue and to seal off blood vessels that are bleeding during surgery. If DR spectroscopy is used in combination with a cauterization instrument, it will be necessary to understand the effects of heat-induced tissue alterations, such as tissue ablation, carbonization, water vaporization, and thermal denaturation of proteins. The need for such smart surgical

instruments is increasing as the standard of care liver surgery tries to spare as much healthy liver tissue as possible, meaning that the number of local and segmental resections increases. Especially with these types of resections, tumor margins are more difficult to judge, especially during laparoscopic liver resection.

5 Conclusion

In summary, in this study, we provided an important validation step for DR spectroscopy-based tissue characterization in liver. We found that bile content can be used as the primary discriminator for transitioning from normal liver tissue to tumor. Given the feasibility of the outlined approach, it is also conceivable to make integrated fiber-optic tools for other oncological procedures that rely on accurate instrument positioning.

Acknowledgments

We thank J. J. J. de Vries, M. Müller, V. V. Pully, C. Reich, and M. van der Voort for their assistance in conducting the clinical experiments. Technical support for this study was provided by Philips Research, Eindhoven, the Netherlands. The authors declare no competing financial interests. The prototype system described in this article is currently only a research prototype and is not for commercial use.

References

1. C. P. Hsu et al., "Liver tumor gross margin identification and ablation monitoring during liver radiofrequency treatment," *J. Vasc. Interv. Radiol.* **16**(11), 1473–1478 (2005).
2. J. W. Spliethoff et al., "Real-time in vivo tissue characterization with diffuse reflectance spectroscopy during transthoracic lung biopsy: a clinical feasibility study," *Clin. Cancer Res.* (2015).
3. A. L. Moreira and R. H. Thornton, "Personalized medicine for non-small-cell lung cancer: implications of recent advances in tissue acquisition for molecular and histologic testing," *Clin. Lung Cancer* **13**(5), 334–339 (2012).
4. B. W. Kuvshinoff and D. M. Ota, "Radiofrequency ablation of liver tumors: influence of technique and tumor size," *Surgery* **132**(4), 605–611; discussion 611–602 (2002).
5. C. R. Buttemere et al., "In vivo assessment of thermal damage in the liver using optical spectroscopy," *J. Biomed. Opt.* **9**(5), 1018–1027 (2004).
6. J. W. Spliethoff et al., "Monitoring of tumor radio frequency ablation using derivative spectroscopy," *J. Biomed. Opt.* **19**(9), 097004 (2014).
7. I. D. Nagtegaal and P. Quirke, "What is the role for the circumferential margin in the modern treatment of rectal cancer?" *J. Clin. Oncol.* **26**(2), 303–312 (2008).
8. R. Nachabé et al., "Effect of bile absorption coefficients on the estimation of liver tissue optical properties and related implications in discriminating healthy and tumorous samples," *Biomed. Opt. Express* **2**(3), 600–614 (2011).
9. D. J. Evers et al., "Optical sensing for tumor detection in the liver," *Eur. J. Surg. Oncol.* **39**(1), 68–75 (2013).
10. R. Nachabé et al., "Real-time in vivo characterization of primary liver tumors with diffuse optical spectroscopy during percutaneous needle interventions: feasibility study in woodchucks," *Invest. Radiol.* **50**(7), 443–448 (2015).
11. W. G. Zijlstra, A. Buursma, and O. W. van Assendelft, *Visible and Near Infrared Absorption Spectra of Human and Animal Haemoglobin*, 1 ed., VSP Publishing, Utrecht (2000).
12. R. Nachabé et al., "Estimation of biological chromophores using diffuse optical spectroscopy: benefit of extending the UV-VIS wavelength range to include 1000 to 1600 nm," *Biomed. Opt. Express* **1**(5), 1432–1442 (2010).
13. R. Nachabé et al., "Estimation of lipid and water concentrations in scattering media with diffuse optical spectroscopy from 900 to 1, 600 nm," *J. Biomed. Opt.* **15**(3), 037015 (2010).
14. M. Fitzmaurice, "Principles and pitfalls of diagnostic test development: implications for spectroscopic tissue diagnosis," *J. Biomed. Opt.* **5**(2), 119–130 (2000).
15. E. Rodriguez-Diaz, I. J. Bigio, and S. K. Singh, "Integrated optical tools for minimally invasive diagnosis and treatment at gastrointestinal endoscopy," *Robot. Comput. Integr. Manuf.* **27**(2), 249–256 (2011).
16. T. J. Farrell, M. S. Patterson, and B. Wilson, "A diffusion theory model of spatially resolved, steady-state diffuse reflectance for the noninvasive determination of tissue optical properties in vivo," *Med. Phys.* **19**(4), 879–888 (1992).
17. D. J. Evers et al., "Diffuse reflectance spectroscopy: towards clinical application in breast cancer," *Breast Cancer Res. Treat.* **137**(1), 155–165 (2013).
18. D. J. Evers et al., "Diffuse reflectance spectroscopy: a new guidance tool for improvement of biopsy procedures in lung malignancies," *Clin. Lung Cancer* **13**(6), 424–431 (2012).
19. J. W. Spliethoff et al., "Improved identification of peripheral lung tumors by using diffuse reflectance and fluorescence spectroscopy," *Lung Cancer* **80**(2), 165–171 (2013).
20. K. Nielsen et al., "The morphological growth patterns of colorectal liver metastases are prognostic for overall survival," *Mod. Pathol.* **27**(12), 1641–1648 (2014).

Biographies for the authors are not available.